Available online at www.sciencedirect.com
ScienceDirect
Trans. Nonferrous Met. Soc. China 26(2016) 1852−1862
Transactions of Nonferrous Metals Society of China
www.tnmsc.cn

Evolving properties of friction stir spot welds between AA1060 and commercially pure copper C11000

Mukuna P. MUBIAYI, Esther T. AKINLABI

Department of Mechanical Engineering Science, Auckland Park Kingsway Campus, University of Johannesburg, Johannesburg 2006, South Africa

Received 23 August 2015; accepted 10 February 2016

Abstract: Friction stir spot welding technique was employed to join pure copper (C11000) and pure aluminium (AA1060) sheets. The evolving properties of the welds produced were characterized. The spot welds were produced by varying the rotational speed, shoulder plunge depth using different tool geometries. The presence of a copper ring of different lengths was observed on both sides of the welds indicating that Cu extruded upward into the Al sheet which contributed to obtaining strong welds. The microstructure showed the presence of copper particles in the aluminium matrix which led to the presence of various intermetallics observed by the energy dispersive spectroscopy and X-ray diffraction. The maximum tensile failure load increases with an increase in the shoulder plunge depth, except for the weld produced at 800 r/min using a conical pin and a concave shoulder. A nugget pull-out failure mode occurred in all the friction stir spot welds under the lap-shear loading conditions. High peaks of Vickers microhardness values were obtained in the vicinity of the keyhole of most of the samples which correlated to the presence of intermetallics in the stir zone of the welds.

Key words: aluminium; copper; friction stir spot welding; microhardness; microstructure

1 Introduction

Among the aims for future years in the automotive industry are the expansion and implementation of new technologies including a broad application of the friction stir spot welding (FSSW) of similar and dissimilar materials. FSSW is a variant of friction stir welding (FSW) for spot welding applications. A non-consumable rotating tool similar to the one used in FSW process is plunged into the workpiece to be joined. Ahead of reaching the desired plunge depth, the rotating tool is held in that position for a fixed period of time, sometimes referred to as the dwell period. Thus, the rotating tool is retracted from the welded joint leaving behind a solid phase joint. During the FSSW, tool penetration and the dwell period basically determine the heat generation, material plasticisation around the pin, the weld geometry and therefore the evolving mechanical properties of the welded joint [1]. A schematic illustration of the FSSW process is shown in Fig. 1 [2].

FSSW process uses a tool, similar to the FSW tool [3]. The shoulder generates the bulk of the friction or deformation heat, whereas, the pin assists in the material flow between the work pieces [1]. Besides the tool, the other parameters which play significant roles in the integrity of the joint formed include the tool rotational speed, the tool plunge depth and the dwell period. These parameters determine the strength and the texture of the weld joints [1,4−6]. There are many published reviews on FSW and FSSW [7−9].

While there are quite a number of published literatures on FSW between aluminium and copper [10−26], few efforts have been made to produce friction stir spot welds between aluminium and copper [27−29]. Yet, the successful friction stir spot welding of these two materials will enhance the usage of friction stir spot welding technology between copper and aluminium which can be used as good replacement for resistance spot welding process in various applications.

ÖZDEMIR et al [27], HEIDEMAN et al [28] and SHIRALY et al [29] have successfully friction stir spot welded a 3 mm-thick AA1050 to pure copper , 1.5 mm thick AA6061-T6 to oxygen free pure copper and 500 μm-thick 1050 aluminum foils to 100 μm-thick pure commercial copper foils (Al/Cu composite), respectively.

Corresponding author: Mukuna P. MUBIAYI; E-mail: patrickmubiayi@gmail.com
DOI: 10.1016/S1003-6326(16)64296-6

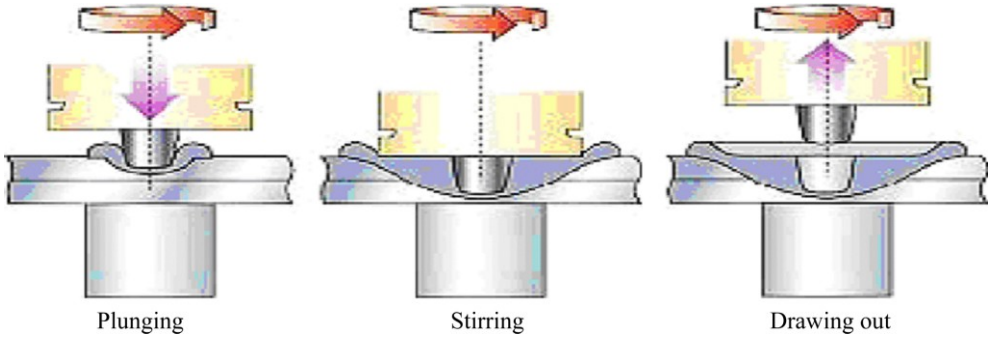

Fig. 1 Schematic illustration of friction stir spot welding process [2]

ÖZDEMIR et al [27] produced friction stir spot welds using three different plunge depths namely 2.8, 4 and 5 mm, using a tool with a shoulder diameter of 20 mm and a pin with a diameter of 5 mm. Furthermore, the spot welds were produced at rotation speed of 1600 r/min for 10 s [27]. The EDS analyses conducted revealed the formation of hard and brittle intermetallic compounds AlCu, Al_2Cu and Al_4Cu_9 formed at the interface [27]. The tensile shear test results showed that 2.8 mm-plunge depth produced poor results whereas 4 mm-plunge depth showed the highest values of shear tensile test compared with the 5 mm-plunge depth, it was suspected to be due to the penetration of Cu into Al in a more diffused way [27]. A maximum hardness value of about HV 160 was obtained in the 4 mm-plunge depth whereas HV 219 was obtained in the 5 mm-plunge depth [27]. However, ÖZDEMIR et al [27] produced welds at 1600 r/min for 10 s dwell time using one tool geometry while in the current study two different tool geometries were used and process parameters were varied.

On the other hand, HEIDEMAN et al [28] conducted metallurgical analysis of AA6061-T6 to oxygen-free Cu using friction stir spot welding process. The tool used was a threaded pin design using a prehardened H13 tool steel with a shoulder of 10 mm, pin diameter of 4 mm and the thread pitch of 0.7 mm. Two different plunge depths of 0 and 0.13 mm were used for two different dwell time of 3 and 6 s [28]. They used rotation speeds varying from 1000 to 2000 r/min. Furthermore, they indicated that, the rotational speed, plunge depth and the tool length were the primary factors affecting the weld strength. The presence of an intermetallic compound was not observed in the high strength welds, they were only in the form of small particles that do not connect along the bond line to become detrimental to the weld quality [28]. SHIRALY et al [29], furthermore, suggested that increasing the maximum shear failure load with the increasing tool rotation rate shows a direct correlation with increasing area and effective length of the stir zone (SZ). Moreover, in all the samples investigated in their study, failure path is through the SZ area. In this context, failure path appears to be an effective parameter on the maximum shear failure load, and the constant failure mode is required to infer that the shear failure strength is only related to the area and effective length of SZ. Furthermore, they obtained the maximum microhardness value of the produced weld in the vicinity of the keyhole.

In the open literature, there is no published work on friction stir spot welds between AA1060 and C11000. Therefore, in this study, FSSW process was used to join C11000 and AA1060. The modification of the evolving microstructural features including fracture mode, height of the extruded copper sheet into the aluminium material produced using different process parameters and tools and their effect on the weld strength were discussed. Furthermore, the analyses of the presence of intermetallic compounds, shear tensile and the Vickers microhardness profiling were also investigated and reported.

2 Experimental

1060 aluminium alloy (AA) and C11000 copper were used for the experiments. The dimensions of the test coupon for each sheet are 600 mm × 120 mm × 3 mm. The weld configuration used in this study is lap joint. The sheets were friction stir spot welded in a 30 mm overlap configuration. The chemical composition of the two parent materials was determined using a spectrometer. Tables 1 and 2 show the chemical composition of AA1060 and C11000, respectively.

The FSS welds were conducted at rotational speeds of 800 and 1200 r/min, the tool shoulder plunge depths

Table 1 Chemical composition of AA1060 (mass fraction, %)

Si	Fe	Ga	Others	Al
0.058	0.481	0.011	0.05	Bal.

Table 2 Chemical composition of C11000 (mass fraction, %)

Zn	Pb	Ni	Al	Co	B	Sb	Nb	Others	Cu
0.137	<0.1	0.02	0.023	0.012	0.077	0.036	0.043	<0.492	Bal.

employed were 0.5 and 1 mm with a constant dwell time of 10 s. The spot welds were produced using an MTS PDS I-Stir at the eNtsa of Nelson Mandela Metropolitan University (NMMU), Port Elizabeth, South Africa. The pin length and the shoulder diameter of the tools were 4 mm and 15 mm, respectively. The tool material is H13 tool steel hardened to HRC 50−52. Two different tool features were used to produce the spot welds, a flat pin and flat shoulder (FPS) and a conical pin and concave shoulder (CCS). The welding process parameters are listed in Table 3.

Table 3 Weld matrix and tool geometries

No.	Shoulder plunge depth/mm	Tool rotational speed/(r·min^{-1})	Shoulder diameter/mm	Tool geometry
1	0.5	800	15	Flat pin and shoulder (FPS)
2	0.5	1200	15	
3	1	800	15	
4	1	1200	15	
5	0.5	800	15	Conical pin and concave shoulder (CCS)
6	0.5	1200	15	
7	1	800	15	
8	1	1200	15	

The shear tensile tests were conducted for all the friction stir spot welded samples by using a tensile testing machine to determine the maximum shear force of the joints. The specimens used in this study for the tensile testing are shown in Fig. 2. The lap shear testing was performed using a 100 kN load cell with a crosshead speed of 3 mm /min.

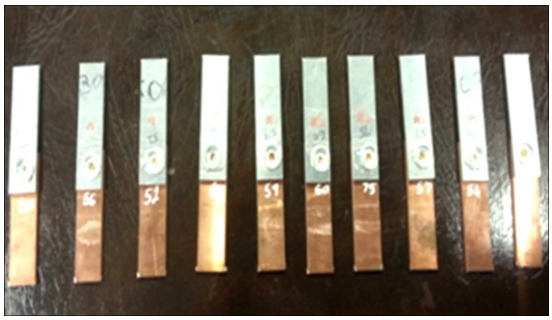

Fig. 2 Tensile shear test specimens

Morphological and qualitative analyses of the spot welds were performed using scanning electron microscopy combined with energy dispersive spectroscopy (SEM/EDS) respectively. Furthermore, X-ray diffraction (XRD) analyses were conducted in the stir zone (SZ) for the qualitative analyses (phase identification) of the possible presence of intermetallics compounds and their compositions. A diffractometer with Cu tube using a recording ranging from 20° to 120° and a step size of 0.04° was used. A 0.8 mm collimator was used for a reliable identification of the phases in the SZ. The Vickers microhardness profiles were measured from the SZ in the middle of the copper ring (top) and in the bottom sheet (copper) as shown in Fig. 3 at a load of 100 g and dwell time of 15 s.

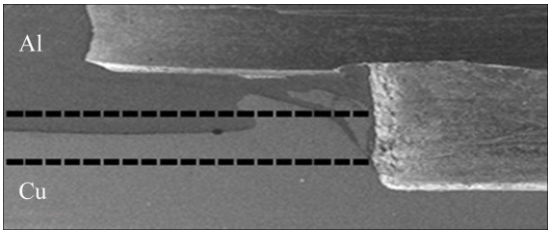

Fig. 3 Typical spot weld with dashed lines illustrating locations of hardness profile measurements

3 Results and discussion

3.1 Macroscopic appearance

Figures 4 and 5 show the macroscopic appearances of the cross-sections of the welds produced using different process parameters and different tools.

It can be seen that the presence of copper rings is evident on both sides of the keyhole, this was also noticed by HEIDEMAN et al [28]. The tool profiles employed to conduct the welds were also clearly visible in the macro appearance.

3.2 Characterisation of copper rings

The presence of copper rings with different lengths was observed in all the spot welds. The copper rings length of the spot welds produced using flat pin and shoulder at 1200 r/min and 1 mm shoulder plunge depth are depicted in Fig. 6.

The formation of the copper rings which consist of the copper parent material extruded in the aluminium sheet can clearly be seen in the produced welds. This can be explained that while the copper material was moving and diffusing into aluminium, aluminium was not diffusing or being pushed into the copper ring [28].

The effect of process parameters and the tool geometries on the penetration length of the copper into aluminium was also studied. The formed copper rings were measured and the results are shown in Figs. 7 and 8 for the flat pin/flat shoulder and the conical pin and concave shoulder respectively.

It was observed that the copper ring length increases with an increase in the shoulder plunge depth, reaches an optimum and then tends to decrease. It has been reported that strong welds were achieved due to the presence of extruded copper upward from the lower

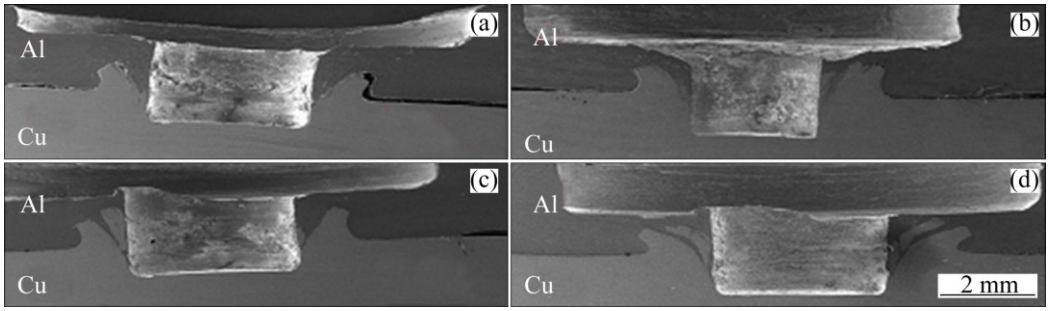

Fig. 4 Micrographs of cross-sections of friction stir spot welds produced by flat pin and shoulder tool: (a) FPS_800_0.5; (b) FPS_800_1; (c) FPS_1200_0.5; (d) FPS_1200_1

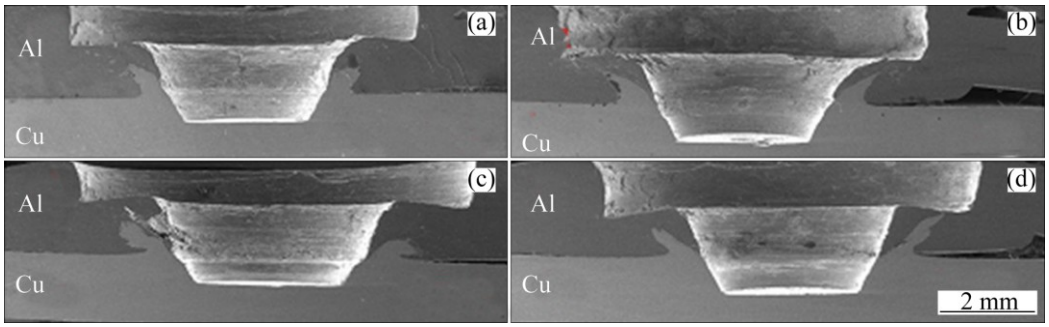

Fig. 5 Micrographs of cross-sections of friction stir spot welds produced by flat pin and shoulder tool: (a) CCS_800_0.5; (b) CCS_800_1; (c) CCS_1200_0.5; (d) CCS_1200_1

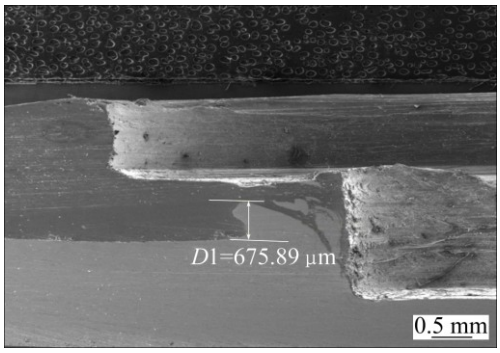

Fig. 6 Copper ring length of spot weld produced at 1200 r/min, 1 mm shoulder plunge depth using flat pin and shoulder tool

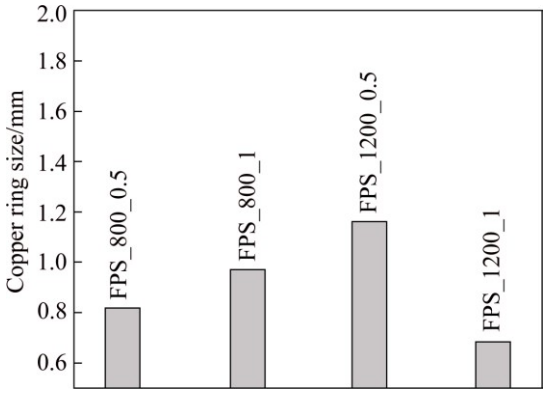

Fig. 7 Copper ring lengths obtained using flat pin and concave shoulder tool at different process parameters

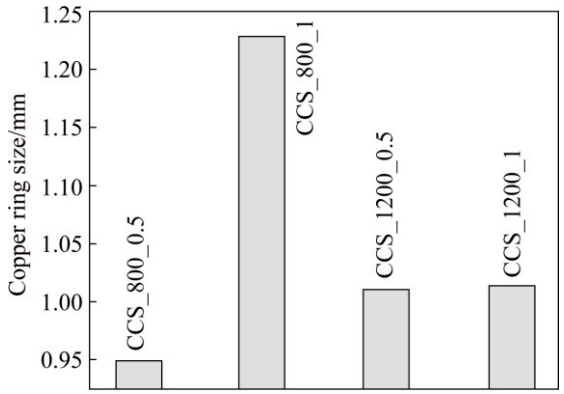

Fig. 8 Copper ring lengths obtained using conical pin and concave shoulder tool at different process parameters

copper sheet into the upper aluminium sheet [28]. The copper ring lengths of the welds produced at 1200 r/min using a conical pin and concave shoulder also has a slight different in the copper ring length. This shows that welds produced at high rotational speed exhibit either a decrease or a slight increment in the copper ring length.

3.3 Scanning electron microscopy and energy dispersive spectroscopy analyses

Figure 9 depicts the SEM secondary electron (SE) and backscattered electron (BSE) micrographs of the copper ring and part of the keyhole at 800 r/min and

0.5 mm shoulder plunge depth.

It can be see from Fig. 9 that the presence of Cu particles into the aluminium matrix which could lead to the formation of hard and brittle intermetallic compounds. To investigate the presence of the intermetallic compounds in the spot welds, energy dispersive spectroscopy (EDS) analyses were carried out in the keyhole and stir zone (SZ). The EDS results indicate the formation of hard and brittle intermetallic compounds. Figures 10 and 11 present the SEM images and EDS analyses for the keyhole and stir zone of the welds produced at 800 r/min, 0.5 mm-shoulder plunge depth and 1200 r/min, 0.5 mm shoulder depth for the flat pin/flat shoulder and conical pin and concave shoulder tool, respectively.

Intermetallic compounds of AlCu, Al_2Cu, $AlCu_3$, Al_2Cu, Al_3Cu_4, Al_2Cu_3 and Al_4Cu_9 were present in the weld samples. The sample produced at 800 r/min, 0.5 mm shoulder plunge depth using a flat pin and flat shoulder showed the presence of AlCu and Al_2Cu in the keyhole, whereas Al_2Cu, Al_4Cu_9 and AlCu intermetallics were found in the stir zone (Fig. 10(a) and Fig. 11(a)). On the other hand, the welds produced at 1200 r/min and 0.5 mm shoulder plunge depth using a conical pin and concave shoulder showed no intermetallics in the keyhole, while Al_2Cu, $AlCu_3$ and AlCu intermetallics were found in the stir zone (Fig. 10(b) and Fig. 11(b)). In various samples, it was noticed that, there was a region rich in aluminium especially in the upper zone (aluminium sheet) of the keyhole with a lower content of copper, this can be attributed to the stirring of the tool pin which took the copper particles from the bottom sheet upward and favoured the presence of either rich-aluminium regions or the presence of intermetallics. This

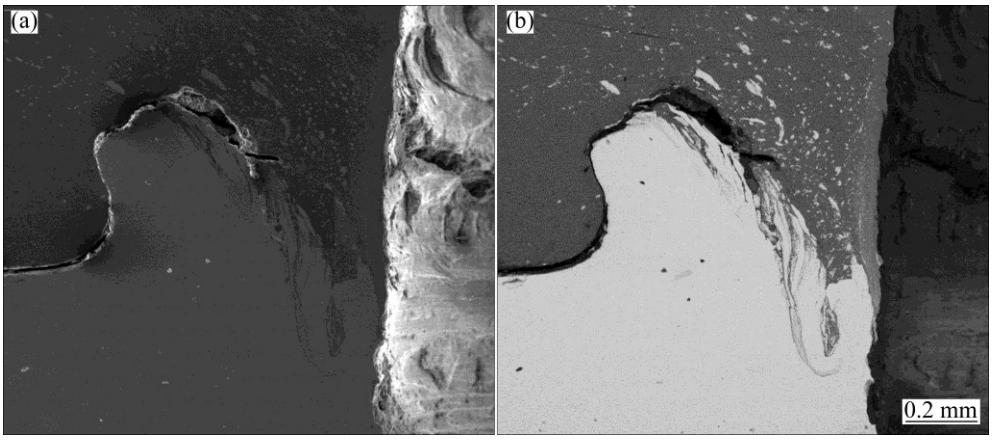

Fig. 9 Secondary electron (a) and backscattered electron (b) images of spot weld produced at 800 r/min and 0.5 mm plunge depth using flat pin and flat shoulder tool

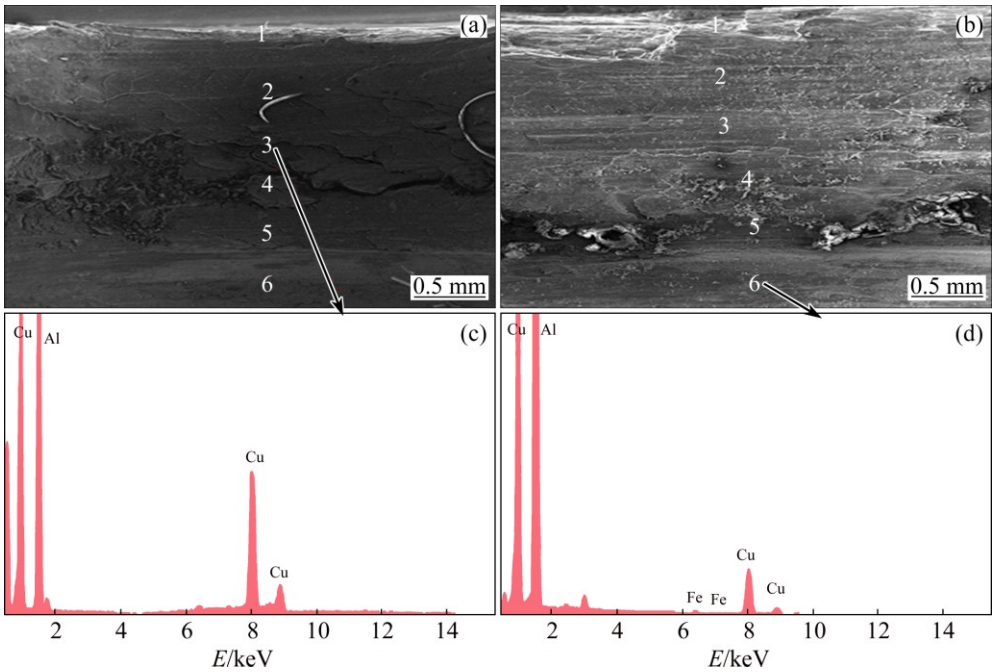

Fig. 10 SEM images of (FPS_800_0.5) (a), (CCS_1200_0.5) (b) welds in keyhole and corresponding EDS analyses (c, d)

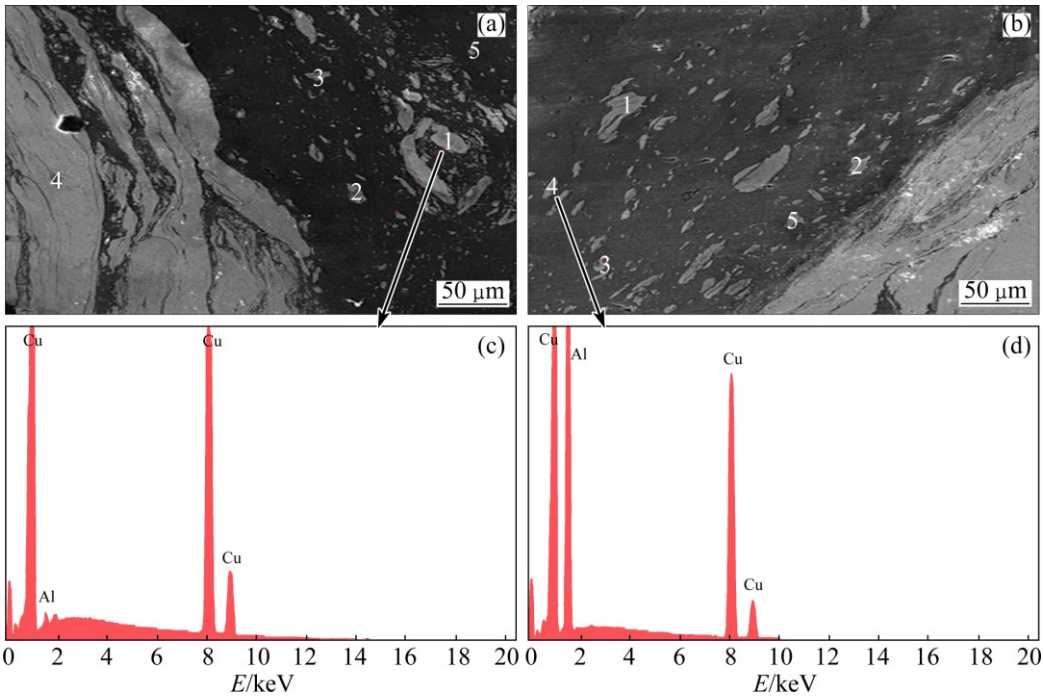

Fig. 11 SEM images of (FPS_800_0.5) (a) and (CCS_1200_0.5) (b) welds in stir zone and corresponding EDS analyses (c, d)

was observed by the decrease in the content of aluminium from the first analyzed point to the last (eventually in the copper where the content of copper increases considerably). This was observed in all the welds except for the weld produced at 1200 r/min, 0.5 mm shoulder plunge depth using a conical pin and concave shoulder.

3.4 X-ray diffraction results

The XRD results of the stir zone of different welds are presented in Table 4.

The XRD patterns obtained in the stir zone show intense aluminium and copper peaks while low intensity XRD peaks depicted the intermetallic compounds. Several authors found the presence of intermetallic compounds in different zones of the welds [10,13,15, 16,29,30]. Due to their low concentrations in different samples, the intermetallics could not be well identified. Similar results were obtained by AKINLABI [10]. Furthermore, intermetallics were found in all the analyzed spot samples. This could be due to the fact that welds were produced at one spot and the amount of heat generated was high which could lead to the formation of intermetallic compounds since they are thermally activated phases [31]. Furthermore, GALVAO et al [13] confirmed the presence of high melting point intermetallic compounds such as Cu_9Al_4 (1030 °C) in the characterised samples using the XRD. They further justified that it was due to the occurrence of the thermomechanically induced solid state diffusion. Typical XRD pattern of the SZ of the weld produced at 800 r/min, 1 mm shoulder plunge depth using flat pin and flat shoulder tool is depicted in Fig. 12.

Table 4 Intermetallic compounds found in stir zone of spot welds samples

Weld	Intermetallic compound
FPS_800_0.5	$AlCu_3$, Al_4Cu_9, Al_2Cu, Al_3Cu_2, Al_2Cu_3, AlCu
FPS_800_1	Al_2Cu, Al_3Cu_2, Al Cu_3
FPS_1200_0.5	Al Cu_3, Al_4Cu_9, Al_2Cu, AlCu
FPS_1200_1	$AlCu_3$, Al_4Cu_9, Al_2Cu, Al_2Cu_3, AlCu
CCS_800_0.5	$AlCu_3$, Al_4Cu_9, Al_2Cu, Al_3Cu_2
CCS_800_1	Al_2Cu, Al_4Cu_9, Cu_3Al, Al_3Cu_2, AlCu, Al_2Cu_3
CCS_1200_0.5	$AlCu_3$, Al_4Cu_9, Al_2Cu, Al_3Cu_2
CCS_1200_1	$AlCu_3$, Al_4Cu_9, Al_2Cu, Al_3Cu_2, AlCu

The diffractograph revealed low peaks for the presence of Al_2Cu, Al_3Cu_2, $AlCu_3$ intermetallics in the SZ, whereas $AlCu_3$, Al_4Cu_9, Al_2Cu and Al_3Cu_2 intermetallics were found in the SZ of the weld produced at 800 r/min, 0.5 mm shoulder plunge depth using a conical pin and concave shoulder as shown in Fig. 13. These results correlated to the results obtained from the EDS which showed the presence of intermetallics in the SZ.

3.5 Shear tests

It has been reported that the presence of the intermetallic compounds at the joint interface could preferentially favour the development of crack during shear tensile analysis [27]. In dissimilar-metal friction

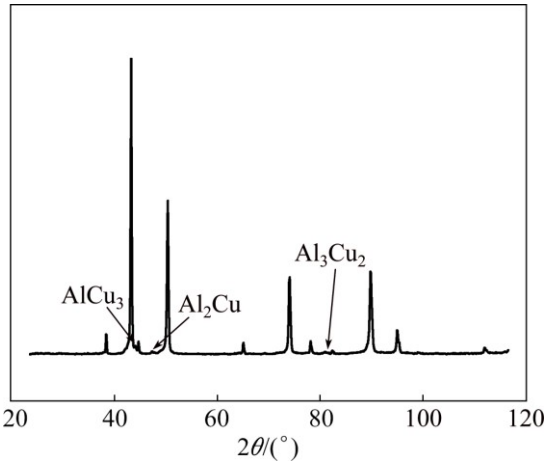

Fig. 12 XRD analysis of stir zone of weld produced at 800 r/min, 1 mm shoulder plunge depth using flat pin and flat shoulder tool

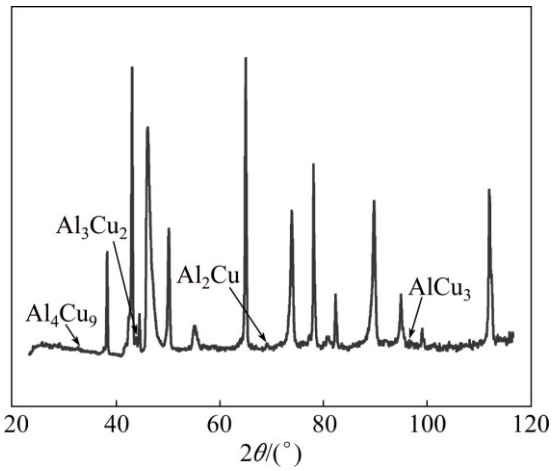

Fig. 13 XRD pattern of stir zone of weld produced at 800 r/min, 0.5 mm shoulder plunge depth using conical pin and concave shoulder tool

stir spot welding (FSSW), intermetallic compounds formation especially in the SZ can significantly reduce the joint strength. High failure loads of 5225 N and 4844 N obtained using a flat pin and flat shoulder were observed at 800 r/min, 1 mm shoulder plunge depth and 1200 r/min and 1 mm shoulder plunge depth, respectively. On the other hand, while using a conical pin and concave shoulder, 4609 N and 4086 N failure loads were obtained for the welds produced at 1200 r/min, 1 mm shoulder plunge depth and 1200 r/min, 0.5 mm shoulder plunge depth, respectively. It was observed that with increasing the plunge depth, welds which could resist high loads were obtained; this was in agreement with results obtained by HEIDEMAN et al [28]. Figure 14 presents some of the shear test results, representing the highest shear loads and displacements curves of the friction stir spot welds using different tool geometries and process parameters.

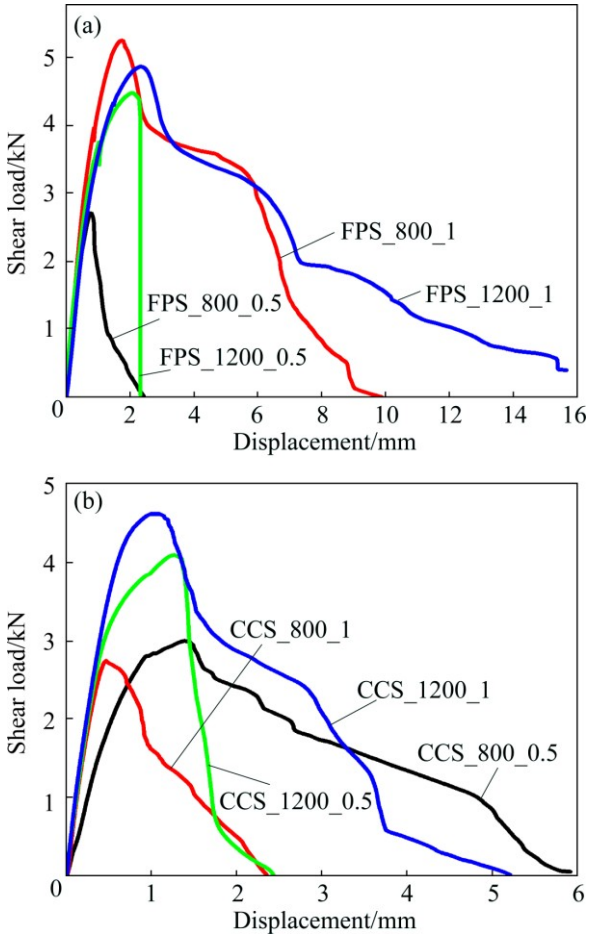

Fig. 14 Load−displacement curves of friction stir spot welds using flat pin and flat shoulder (a) and conical pin and concave shoulder (b)

Moreover, the presence of the copper ring extruded upward on both side of the keyhole from the lower copper sheet was suspected to influence the fracture mode. The copper ring caused interlocking between the two sheets and helped the sheets adhere to each other during tensile testing to reach a high strength before failure [28]. The effects of the process parameters on the maximum failure load are depicted in Fig. 15 for the welds produced using a flat pin/ flat shoulder and conical pin and concave shoulder.

It was observed that as the shoulder plunge depth increases, the failure load increases, except for the weld produced at 800 r/min using a conical pin and concave shoulder.

3.6 Analyses of fracture mode

According to the study conducted by LIN et al [32], the shear failure mechanism is the principal failure initiation mechanism of the nugget pull out failure mode in lap-shear specimens from the mechanics point of view. Only one fracture mode was observed in all the analysed samples as shown in Figs. 16 (a) and (b).

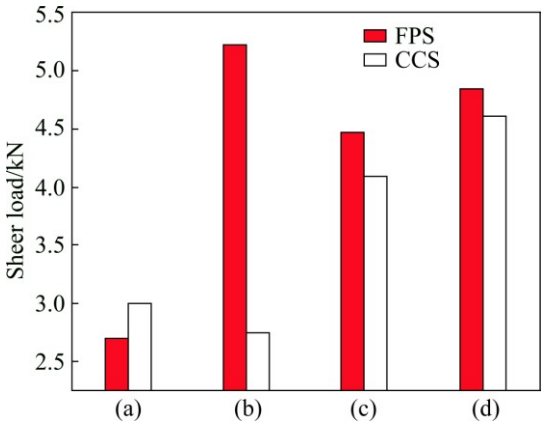

Fig. 15 Effect of process parameters on maximum failure load of welds: (a) 800 r/min, 0.5 mm shoulder plunge depth; (b) 800 r/min, 1 mm shoulder plunge depth; (c) 1200 r/min, 0.5 mm shoulder plunge depth; (d) 1200 r/min, 1 mm shoulder plunge depth

Only the pull nugget failure mode was observed. This was due to the difference in the properties of the parent materials which could be explained by the presence of the copper rings. The fracture surface of the spot weld made using a flat pin and flat shoulder tool at a rotation speed of 800 r/min and the shoulder plunge depth of 0.5 mm, was observed using scanning electron microscopy, as shown in Figs. 16 (c) and (d), which revealed a ductile morphology. The dimples were in different sizes as depicted in Figs. 16 (c) and (d), this can be attributed to the effect of the different process parameters and tool geometries used. It can also be seen that the prominent fracture surface includes small dimples which can be attributed to the homogeneous microstructure of the small grains at the failure location [33].

3.7 Vickers microhardness profiling

The microhardness values of the parent materials are in the range of HV 86.7−HV 96.3 for Cu, whereas, for Al, the range is HV 34.6−HV 40.3. In all the samples, high microhardness values were recorded at the top in the region close to the keyhole. It has been reported that the presence of hard and brittle intermetallic compounds causes the sudden increase of microhardness in the stir zone [29]. Furthermore, SHIRALY et al [29] stated that the higher microhardness values around the keyhole have good consistency with the Cu layers severely broken up into fine particles that are randomly dispersed. However, microhardness was high possibly due to the presence of intermetallic compounds [29]. These statements were in agreement with the results obtained in the current study. The XRD analyses of the SZ revealed the presence of hard and brittle intermetallic compounds including $CuAl_2$, Al_3Cu_2, Cu_3Al, Al_4Cu_9 and AlCu. This was further confirmed with the energy dispersive spectroscopy conduced in the SZ. The highest microhardness values of HV 63.8, HV 415, HV 153 and HV 154 were obtained at the top side of the samples for FPS_800_0.5, FPS_800_1, FPS_1200_0.5 and FPS_1200_1, respectively (Fig. 17(a)). While, the

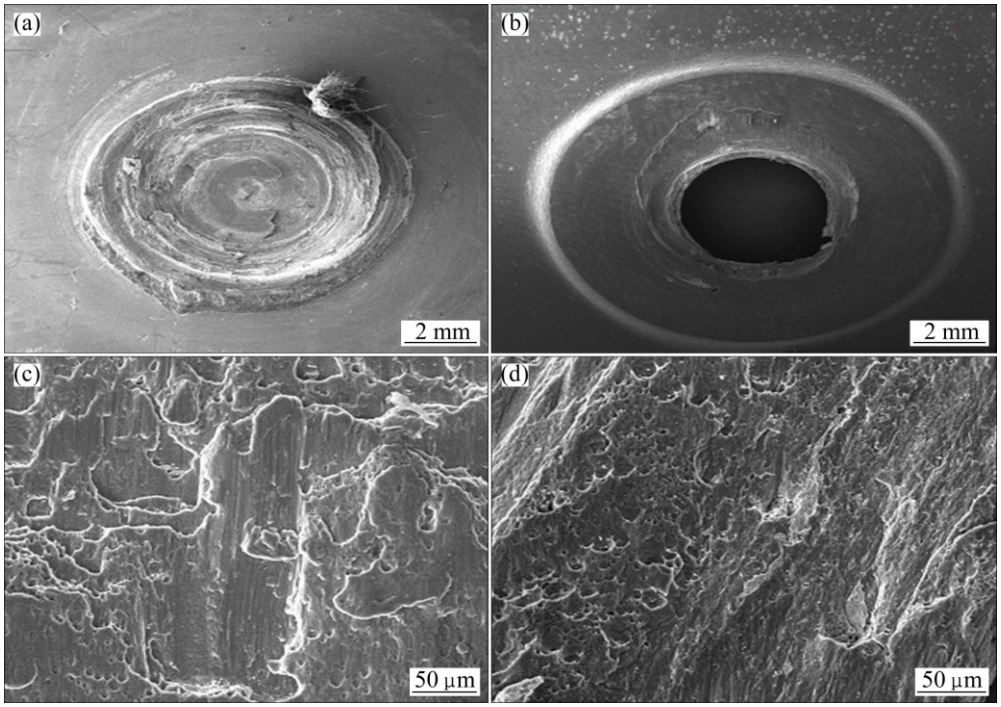

Fig. 16 SEM images of spot weld produced using flat pin and flat shoulder tool with rotation speed of 800 r/min and shoulder plunge depth of 0.5 mm: (a) Failed nugget lower sheet (Cu); (b) Upper sheet (Al); (c, d) Fracture surfaces on copper and aluminium side, respectively

microhardness values of HV 105, HV 158, HV 94.4, and HV 96 were found at the bottom measurements of the same samples as illustrated in Fig. 17(b).

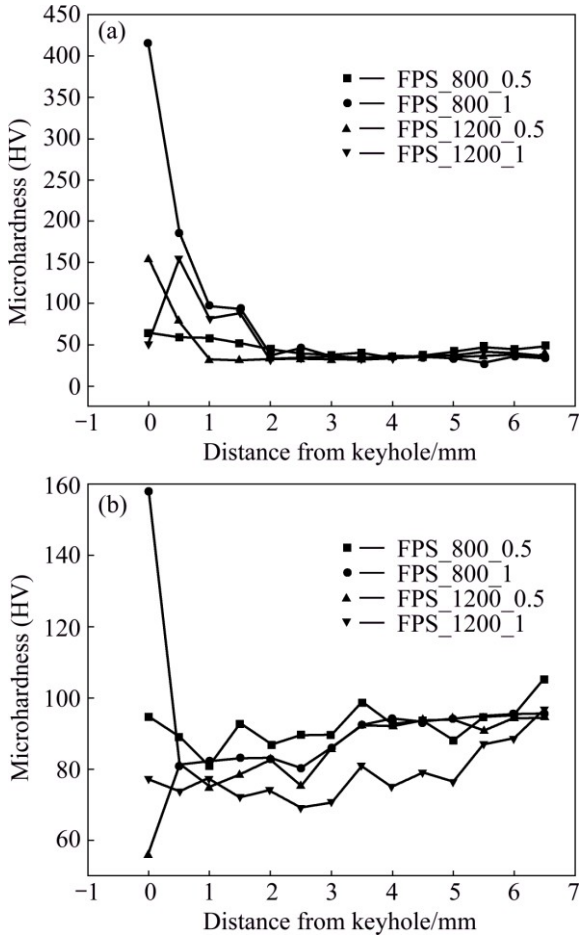

Fig. 17 Microhardness distribution along welds produced using flat pin and flat shoulder tool with different process parameters: (a) Top; (b) Bottom

On the other hand, the maximum microhardnesses of HV 123, HV 140, HV 109, and HV 93.3 were obtained at the top for CCS_800_0.5, CCS_800_1, CCS_1200_0.5 and CCS_1200_1, respectively (Fig. 18(a)). Whereas, microhardness values of HV 95. 7, HV 101, HV 96 and HV 96.1 were obtained at bottom measurements of the same samples as shown in Fig. 18(b).

Furthermore, all the microhardness values recorded in the regions close to the keyhole for all the spot welds produced using a conical pin and concave shoulder (bottom) have lower values which were close to the average value of the copper base material; the microhardness values increase with the increase of the distance from the keyhole. This was due to the presence of the aluminium particle mixed with copper particles in that region close to the copper sheet. The aluminium particles were pushed down into the vicinity of copper sheet during the tool rotation movement.

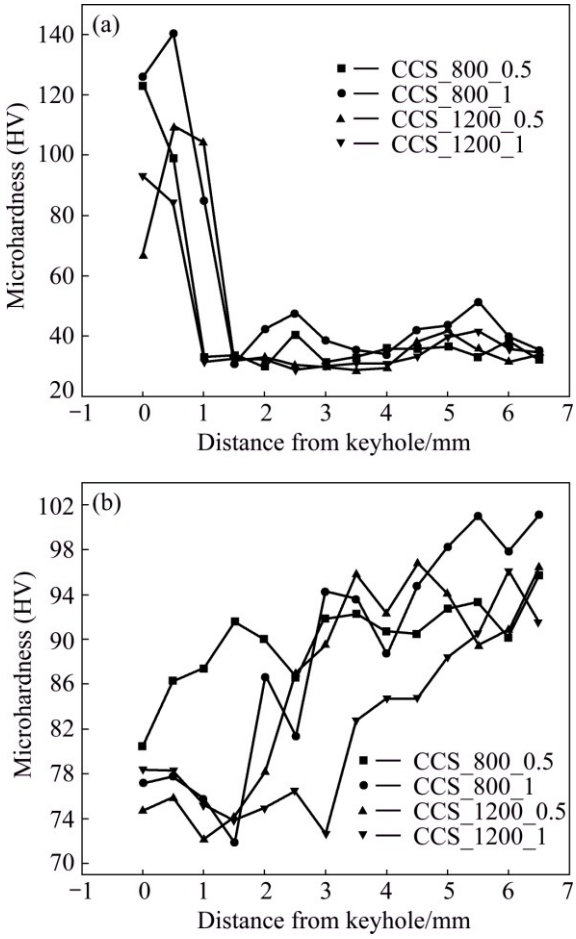

Fig. 18 Microhardness distribution along welds produced using conical pin and concave shoulder at different process parameters: (a) Top; (b) Bottom

It was further observed that the shoulder plunge depth had an effect on the microhardness of all the samples except the spot weld produced at 1200 r/min and 1 mm shoulder plunge depth, where a decrease was observed for the measurement carried out at the top of the samples. As for the bottom measurements, similar observation was noticed (Figs. 19 and 20).

4 Conclusions

1) The presence of a copper ring was observed in both sides of the welded samples. The copper rings consisted of the copper parent material extruded in the aluminium sheets. The length of the copper rings was measured and was observed that the length of the copper rings increased with the increase of the shoulder plunge depths up to an optimum and then tended to decrease as the rotational speed increased. It was further observed that the length of the copper rings in the welds produced at 1200 r/min exhibited either a decrease or a small increase.

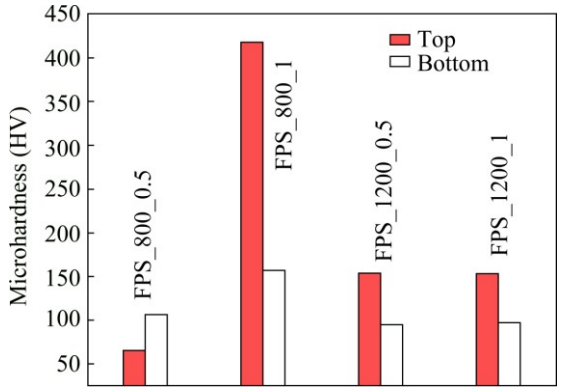

Fig. 19 Variation of maximum microhardness values obtained at different process parameters and locations

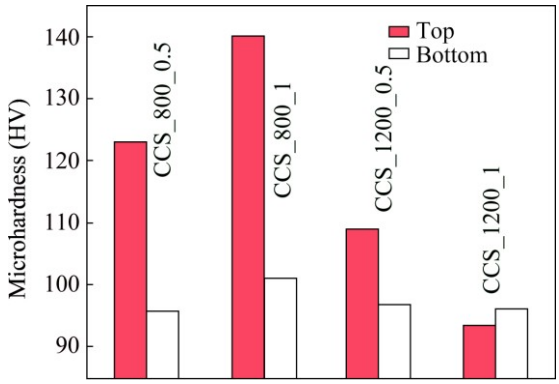

Fig. 20 Variation of maximum microhardness values obtained at different process parameters and locations

2) The EDS analyses of the keyhole and SZ revealed the presence of intermetallic compounds of AlCu, Al_2Cu, $AlCu_3$, Al_2Cu, Al_3Cu_4, Al_2Cu_3 and Al_4Cu_9 in the spot welds in low concentrations. This was further confirmed with the XRD analyses of the SZ which also showed the presence of the intermetallics.

3) The lowest and the highest failure loads were obtained for the welds produced at 800 r/min, 0.5 mm shoulder plunge depth and 800 r/min, and 1 mm shoulder plunge depth, respectively. Both welds were produced using a flat pin and flat shoulder tool. Furthermore, only a pull nugget failure mode was observed in all the welds.

4) The microhardness values recorded at the top were high in all the samples, which were found in the region close to the keyhole. Furthermore, all the microhardness values recorded at the bottom of the samples in the region close to the keyhole for all the spot welds produced using a conical pin and concave shoulder had lower values which were close to the average value of the copper base material. In this study, an optimum parameter combination setting of 800 r/min and 1 mm shoulder plunge depth using a flat pin and flat shoulder tool can be recommended.

Acknowledgments

The financial support of the University of Johannesburg and the assistance from Mr Riaan Brown (Nelson Mandela Metropolitan University) for operating the MTS PDS I-Stir machine are acknowledged.

References

[1] THOMAS W M, NICHOLAS E D, NEEDHAM J C, MURCH M G, TEMPLE-SMITH P, DAWES C J. Friction stir butt welding: PCT/GB92/02203 [P]. 1991.

[2] MERZOUG M, MAZARI M, BERRAHAL L, IMAD A. Parametric studies of the process of friction spot stir welding of aluminium 6060-T5 alloys [J]. Materials and Design, 2010, 31: 3023−3028.

[3] BADARINARAYAN H. Fundamentals of friction stir spot welding [D]. Rolla: Missouri University of Science and Technology, 2009.

[4] BOZKURT Y, SALMAN S, ÇAM G. Effect of welding parameters on lap shear tensile properties of dissimilar friction stir spot welded AA 5754-H22/2024-T3 joints [J]. Science and Technology of Welding and Joining, 2013, 18(4): 337−345.

[5] IPEKOGLU G, ÇAM G. Effects of initial temper condition and postweld heat treatment on the properties of dissimilar friction-stir-welded joints between AA7075 and AA6061 aluminum alloys [J]. Metallurgical and Materials Transactions A, 2014, 45(7): 3074−3087.

[6] ÇAM G, IPEKOGLU G, TARIK SERINDAG H. Effects of use of higher strength interlayer and external cooling on properties of friction stir welded AA6061-T6 joints [J]. Science and Technology of Welding and Joining, 2014, 19(8): 715−720.

[7] ÇAM G. Friction stir welded structural materials: Beyond Al-alloys [J]. International Materials Reviews, 2011, 56(1): 1−48.

[8] ÇAM G, MISTIKOGLU S. Recent developments in friction stir welding of Al-alloys [J]. Journal of Materials Engineering and Performance, 2014, 23 (6): 1936−1953.

[9] MUBIAYI M P, AKINLABI E T. An overview on friction stir spot welding of dissimilar materials [M]//Transactions on Engineering Technologies 2014, IAENG, Springer Dordrecht Heidelberg New York London, 2015: 537−549.

[10] AKINLABI E T. Characterisation of dissimilar friction stir welds between 5754 aluminium alloy and C11000 copper [D]. South Africa: Nelson Mandela Metropolitan University, 2010.

[11] GALVAO I, LEAL R M, RODRIGUEZ D M, LOUREIRO A. Dissimilar welding of very thin aluminium and copper plates [C]//Proceedings of 8th International Friction Stir Welding Symposium. Germany: Timmendorfer Strand, 2010: 992−1008.

[12] SAEID T, ABDOLLAH-ZADEH A, SAZGARI B. Weldability and mechanical properties of dissimilar aluminum–copper lap joints made by friction stir welding [J]. Journal of Alloys and Compounds, 2010, 490: 652−655.

[13] GALVAO I, OLIVEIRA J C, LOUREIRO A, RODRIGUES D M. Formation and distribution of brittle structures in friction stir welding of aluminium and copper: Influence of process parameters [J]. Science and Technology of Welding and Joining, 2011, 16(8): 681−689.

[14] ESMAEILI A, BESHARATI GIVI M K, ZAREIE RAJANI H R. A metallurgical and mechanical study on dissimilar friction stir welding of aluminum 1050 to brass (CuZn30) [J]. Materials Science and Engineering A, 2011, 528: 7093−7102.

[15] XUE P, NI D R, WANG D, XIAO B L, MA Z Y. Effect of friction stir welding parameters on the microstructure and mechanical properties of the dissimilar Al−Cu joints [J]. Materials Science and Engineering A, 2011, 528: 4683−4689.

[16] XUE P, XIAO B L, WANG D, MA Z Y. Achieving high property friction stir welded aluminium/copper lap joint at low heat input [J]. Science and Technology of Welding and Joining, 2011, 16(8):

657−661.
[17] AVETTAND-FENOE M N L, TAILLARD R, JI G, GORAN D. Multiscale study of interfacial intermetallic compounds in a dissimilar Al 6082-T6/Cu friction-stir weld [J]. Metallurgical and Materials Transactions A, 2012, 43: 4655−4666.
[18] AKINLABI E T. Effect of shoulder size on weld properties of dissimilar metal friction stir welds [J]. Journal of Materials Engineering and Performance, 2012, 21(7): 1514−1519.
[19] SINGH R K R, PRASAD R, PANDEY S. Mechanical properties of friction stir welded dissimilar metals [C]//Proceedings of the National Conference on Trends and Advances in Mechanical Engineering. Faridabad, Haryana, YMCA University of Science & Technology, 2012: 579−583.
[20] AGARWAL P, NAGESWARAN P, ARIVAZHAGAN N. RAMKUMAR K D. Development of friction stir welded butt joints of AA 6063 aluminium alloy and pure copper [C]//International Conference on Advanced Research in Mechanical Engineering, Naintal, Uttarakhand, India: IPM rt. Ltd, 2012: 46−50.
[21] BISADI H, TAVAKOLI A, TOUR SANGSARAKI M, TOUR SANGSARAKI K. The influences of rotational and welding speeds on microstructures and mechanical properties of friction stir welded Al5083 and commercially pure copper sheets lap joints [J]. Materials and Design, 2013, 43: 80−88.
[22] MUTHU M F X, JAYABALAN V. Tool travel speed effects on the microstructure of friction stir welded aluminium−copper joints [J]. Journal of Materials Processing Technology, 2015, 217: 105−113.
[23] LI Xia-wei, ZHANG Da-tong, QIU Cheng, ZHANG Wen. Microstructure and mechanical properties of dissimilar pure copper/1350 aluminum alloy butt joints by friction stir welding [J]. Transactions of Nonferrous Metals Society of China, 2012, 22(6): 1298−1306.
[24] AKINLABI E T, ANDREWS A, AKINLABI S A. Effects of processing parameters on corrosion properties of dissimilar friction stir welds of aluminium and copper [J]. Transactions of Nonferrous Metals Society of China, 2014, 24(5): 1323−1330.
[25] BHATTACHARYA T K, DAS H, PAL T K. Influence of welding parameters on material flow, mechanical property and intermetallic characterization of friction stir welded AA6063 to HCP copper dissimilar butt joint without offset [J]. Transactions of Nonferrous Metals Society of China, 2015, 25(9): 2833−2846.
[26] ZHANG Qiu-zheng, GONG Wen-biao, LIU Wei. Microstructure and mechanical properties of dissimilar Al−Cu joints by friction stir welding [J]. Transactions of Nonferrous Metals Society of China, 2015, 25(6): 1779−1786.
[27] ÖZDEMIR U, SAYER S, YENI Ç, BORNOVA-IZMIR. Effect of pin penetration depth on the mechanical properties of friction stir spot welded aluminum and copper [J]. Materials Testing in Joining Technology, 2012, 54(4): 233−239.
[28] HEIDEMAN R, JOHNSON C, KOU S. Metallurgical analysis of Al/Cu friction stir spot welding [J]. Science and Technology of Welding and Joining, 2010, 15(7): 597−604.
[29] SHIRALY M, SHAMANIAN M, TOROGHINEJAD M R, AHMADI JAZANI M. Effect of tool rotation rate on microstructure and mechanical behavior of friction stir spot-welded Al/Cu composite [J]. Journal of Materials Engineering and Performance, 2014, 23(2): 413−420.
[30] XUE P, XIAO B L, NI D R, MA Z Y. Enhanced mechanical properties of friction stir welded dissimilar Al−Cu joint by intermetallic compounds [J]. Materials Science and Engineering A, 2010, 527: 5723−5727.
[31] ABDOLLAH-ZADEH A, SAEID T, SAZGARI B. Microstructural and mechanical properties of friction stir welded aluminum/copper lap joints [J]. Journal of Alloys and Compounds, 2008, 460: 535−538.
[32] LIN P C, LIN S H, PAN J. Modeling of plastic deformation and failure near spot welds in lap shear specimens [J]. Sae Technical Papers, 2004, doi: 10.4271/2004-01-0817.
[33] LINA YU , KAZUHIRO NAKATA , JINSUN LIAO. Microstructural modification and mechanical property improvement in friction stir zone of thixo-molded AE42 Mg alloy [J]. Journal of Alloys and Compounds, 2009, 480(2): 340−346.

AA1060 铝合金和 C1100 工业纯铜搅拌摩擦点焊的演变性能

Mukuna P. MUBIAYI, Esther T. AKINLABI

Department of Mechanical Engineering Science, Auckland Park Kingsway Campus, University of Johannesburg, Johannesburg 2006, South Africa

摘　要：采用搅拌摩擦点焊技术连接纯铜(C11000)和纯铝(AA1060)板材，并表征了焊缝的演变性能。在不同转速和送入深度下，采用不同形状刀具制备点焊焊缝。在焊缝两边可观察到不同长度铜环，这表明铜向前挤压进入铝板，有助于得到高强焊缝。采用能量散射谱和 X 射线衍射研究手段可观察到在铝基体中存在铜粒子，且有各种不同的金属间化合物存在。除了在转速 800 r/min 下采用锥形销和凹形肩得到的焊缝外，最大的拉伸断裂载荷随着送入深度的增加而增大。在剪切−拉伸载荷条件下，所有的搅拌摩擦点焊接头产生了点焊熔核滑脱失效模式。在样品锁眼附近得到了峰值硬度，这同焊接搅拌区存在金属间化合物有关。

关键词：铝；铜；搅拌摩擦点焊，显微硬度；显微组织

(Edited by Xiang-qun LI)